Numerical Investigation of the Effect of Conjugate Heat Transfer on Sulfuric Acid Condensation in a Large Two-Stroke Marine Diesel Engine

Jensen, M. V.; Karvounis, N.; Pang, K. M.; Ong, J. C.; Schramm, J.; Walther, J. H.

Publication date:
2019

Document Version
Peer reviewed version

NUMERICAL INVESTIGATION OF THE EFFECT OF CONJUGATE HEAT TRANSFER ON SULFURIC ACID CONDENSATION IN A LARGE TWO-STROKE MARINE DIESEL ENGINE

Jensen M. V.*, Karvounis N., Pang K. M., Ong J. C., Schramm, J. and Walther J. H.
*Author for correspondence
Department of Mechanical Engineering,
Technical University of Denmark,
2800 Kgs. Lyngby
Denmark,
E-mail: mvje@mek.dtu.dk

ABSTRACT

Sulfuric acid condensation on liner walls in large two-stroke marine diesel engines may lead to cold corrosion and hence excessive liner wear rates. Understanding of the phenomenon and factors influencing it is therefore important. In this study we present results from a numerical investigation of sulfuric acid and water vapor condensation in a large two-stroke marine diesel engine using computational fluid dynamics (CFD) incorporating conjugate heat transfer modeling between the cylinder gas and liner wall. The combustion phase of the engine cycle is simulated using a reduced n-heptane chemical kinetic mechanism including a sulfur chemistry subset for modeling the formation of sulfur oxides and subsequently sulfuric acid vapor. Condensation of sulfuric acid and water vapor on the cylinder liner is evaluated by determining if the local liner temperature is below the local dew point of sulfuric acid and water, respectively. A layer of 25 solid cells is added on the cylinder liner to represent the liner material for the implementation of conjugate heat transfer calculations between the cylinder gas and liner. The thickness of the cell layer is 5 mm, and we use a temperature boundary condition on the backside of the cell layer based on experimental measurements. We compare the obtained results with results where conjugate heat transfer calculations are not considered, and the influence on the results is evaluated to determine the importance of incorporating the interrelated thermal dynamics of the combustion gas-solid wall system.

INTRODUCTION

Due to increasing oil prices and environmental concern slow steaming operation was introduced and became widely applied worldwide in the maritime industry about 10 years ago [1]. The slow steaming operation mode, i.e. to sail slower, leads to a significantly lower drag force on the ship hull than at full speed operation since the drag force scales with the velocity squared. The needed propulsion power scales with the cube of the velocity, not linearly, and hence a significant fuel saving is obtained at slow steaming operation. An unwanted side effect of slow steaming is however a higher risk of increased cylinder liner wear rates in the ship propulsion engines [2,3]. When slow steaming, the propulsion engine is typically operated at low load conditions. Due to less fuel burned at low load operation the heat transfer to the combustion chamber surfaces decreases and hence the cylinder liner temperature becomes lower than at full load operation. The fuel oil applied in the engines contains sulfur, and sulfur oxides are formed during combustion. Near the cylinder liner the sulfur oxides reacts with water vapor and forms sulfuric acid. Lower liner temperatures may lead to increased condensation of sulfuric acid on the liner and subsequent sulfuric acid corrosion. At the same time an increased combustion pressure in the cylinder as a result of engine development leads to higher partial pressures of sulfuric acid and water vapor and hence higher dew points. Sulfuric acid corrosion is suspected to be a main reason for increased liner wear rates at slow steaming operation. Increased condensation of water vapor on the liner leading to water corrosion may also contribute to the increased wear rates as ships operating in humid conditions experience higher liner wear rates. Current research at the Technical University of Denmark using a novel cold corrosion test engine supports this since results indicate that water condensation on a cylinder liner can significantly increase the liner wear [3]. Condensation of sulfuric acid or water vapor on the engine cylinder liner will occur if the local temperature is below the local dew point of sulfuric acid or water, respectively. The liner surface temperature varies with location and time due to spatial and temporal variation in the gas temperature. At the same time the local concentration of sulfuric acid and water vapor varies spatially and temporally, and hence does the local dew point of these two species. These factors make the determination of the total sulfuric acid and water vapor condensation in the engine a complex task as well as estimating the liner area which is affected. Numerical investigations applying computational fluid dynamic (CFD) simulations may provide valuable information in this respect. However, CFD simulation studies of large two-stroke marine engines are limited in the open literature. Pang et al. [4] performed a numerical work on sulfur oxides formation during combustion in a large two-stroke marine diesel engine with subsequent formation of sulfuric acid. They established a 3D CFD engine model which applies a reduced sulfur chemical kinetic mechanism combined with a skeletal n-heptane mechanism. The basis for the model is the 4T50ME-X low speed two-stroke test engine located at MAN Energy Solutions, Denmark. Model predictions of the sulfur oxides were evaluated

using measurements. Karvounis et al. [5] further developed the engine model established by Pang et al. [4] by including a condensation model coupled with a fluid film model for simulating condensation of sulfuric acid and water vapor on the cylinder liner. The condensation of the two species was investigated for different engine operating conditions including scavenging air pressure and humidity, as well as fuel sulfur content and cylinder liner temperature. The investigations in both [4] and [5] applied a constant and uniform cylinder liner surface temperature of 50°C or 250°C as thermal wall boundary condition. The liner surface temperature of engines varies however, as mentioned, with location and time which may influence the condensation of sulfuric acid and water vapor on the liner. Therefore, in the present study we examine the influence of a spatially and temporally varying cylinder liner surface temperature on the condensation. This is performed by including a solid region representing the cylinder liner in the CFD model of Pang et al. [4]. On the backside of the solid region a fixed temperature is imposed while the liner surface temperature at the interface with the cylinder gas is determined based on conjugate heat transfer (CHT) calculations.

NOMENCLATURE

A	[m^2]	Area
c	[J/(kg K)]	Specific heat capacity
F_s	[-]	Liner surface area fraction exposed to possible condensation
p_a	[mmHg]	Partial pressure of sulfuric acid
p_w	[mmHg] or [Pa]	Partial pressure of water
$T_{DP,a}$	[K]	Dew point of sulfuric acid
$T_{DP,w}$	[K]	Dew point of water
T_w	[K]	Wall temperature
Special characters		
α	[m^2/s]	Thermal diffusivity
λ	[W/(m K)]	Thermal conductivity
ρ	[kg/m^3]	Density
ϕ	[-]	Parameter that assumes a value of 1 or 0

NUMERICAL MODEL

The numerical model applied in the present investigation is a 3D CFD engine model set up in the commercial CFD code STAR-CCM+ version 13.06.012-R8 [6]. The model is an extended version of the model reported in [4] and [5] which simulates the 4T50ME-X low speed two-stroke MAN test engine. The main engine specifications are shown in Table 1.

Bore	500 mm
Stroke	2200 mm
Connecting rod length	2885 mm
Number of fuel injectors	2

Table 1 Main specifications for the 4T50ME-X engine.

Governing equations, turbulence and combustion modeling

The governing equations are the Unsteady Reynolds-Averaged Navier-Stokes (URANS) equations, and turbulence is modelled using the k-ω SST eddy viscosity model. An Eulerian-Lagrangian formulation is applied for the fuel injection and combustion process where the fuel is represented as liquid droplets that subsequently break up and evaporate. Combustion reactions are modelled using a skeletal n-heptane chemical kinetic mechanism combined with a sulfur chemistry subset to account for sulfur oxides formation and subsequently formation of sulfuric acid vapor. The complete mechanism consists of 37 species and 77 reactions, and is coupled to the 3D CFD model via the DARS-CFD solver [6]. For further information on the model setup and model validation, see [4]. The current model in the present study does not include the condensation and fluid film models described in [5] due to present complications in combining them with the implementation of the solid region representing the cylinder liner. Instead the dew points of sulfuric acid and water are used in the current model to estimate if condensation on the cylinder liner potentially occurs.

Geometry and computational mesh

The present investigation considers the closed part of the engine cycle and only one cylinder. The simulation starts with the piston at top dead center (TDC) and continues until 90 crank angle degrees (CAD) after top dead center (ATDC). Therefore, no scavenge ports, scavenge box or exhaust gas receiver is included in the model geometry which only comprise the combustion chamber and a part of the cylinder liner. Since the cylinder is equipped with two fuel injectors symmetrically located, a sector mesh of 180° is used with cyclic boundary conditions on the intersection plane. The piston, cylinder head and exhaust valve are modelled as plane geometries for simplicity. The model geometry with the piston at TDC is show in Figure 1.

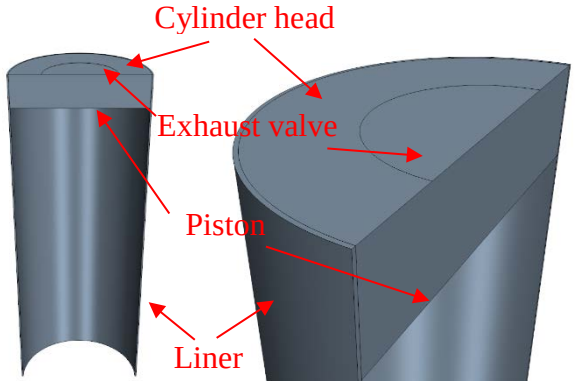

Figure 1 Model geometry with piston at TDC.

The computational mesh for the combustion chamber is structured with mesh refinements near walls and local refinement in the spray and combustion region. The mesh is the same as that used in [5] which is based on [4]. We refer to these references for detailed information on the mesh.

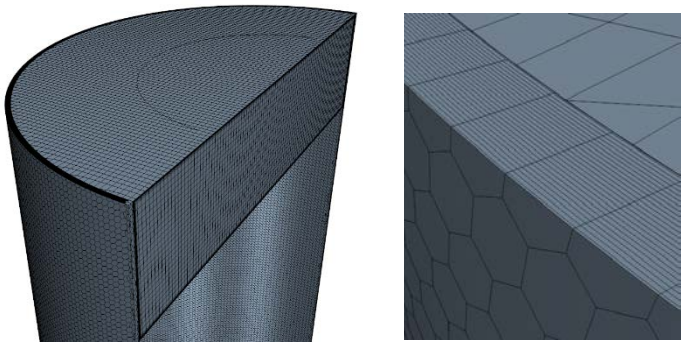

Figure 2 Computational mesh with piston at TDC (left) and zoom on cylinder liner mesh (right).

A cell layer of 5 mm is included in the model to represent a part of the cylinder liner. The layer consists of 25 solid cells in radial direction. The solid material is cast iron with a specific heat capacity of c = 476 J/(kg K), a thermal conductivity of λ = 51 W/(m K), and a density of ρ = 7320 kg/m^3 resulting in a thermal diffusivity of $\alpha = \lambda/(\rho\ c) = 1.46 \cdot 10^{-5}$ m^2/s. In a previous numerical investigation [7], it was indicated that temperature oscillations into the piston crown material are dampened out within 5 mm below the surface. A steel alloy was used for the piston crown material in [7] with a thermal diffusivity of $\alpha = 8.70 \cdot 10^{-6}$ m^2/s. Although the thermal diffusivity of the liner is almost a factor two higher we use a cell layer thickness for the liner of also 5 mm due to liner temperature measurements in about this depth which is used as boundary condition in the model. If the temperature oscillations have been dampened out within this depth is not known but could be indicated by performing consecutive full cycle simulations with the model. However, due to time restrictions, this has not been possible in the present investigation and is left for a future study. The computational mesh is shown in Figure 2. The total cell number in the model is 1.58×10^6 cells.

Boundary and initial conditions

Wall boundary conditions with a fixed temperature are imposed on the surface of the piston (400°C), cylinder head (250°C) and exhaust valve (600°C), and on the backside of the liner cell layer (50°C). Adiabatic wall boundary conditions are imposed on the top and lower face of the liner cell layer, and cyclic boundary conditions are imposed on the intersection plane of the cylinder gas cells and the liner cell layer. The initial conditions for the simulation are given in Table 3 and are based on conditions in [4] and [8]. The engine speed is 123 rpm.

Gas temperature	651 °C
Pressure	151.9 bar
Velocity field	See [8]
Turbulence field	See [8]
Liner temperature	50 °C
Crank angle degree	0 (TDC)

Table 2 Imposed initial conditions at TDC.

Conjugate heat transfer calculations

The CHT calculations in the present study are performed by formulating and solving the energy equation for both the cylinder gas and the liner with a thermal coupling imposed at the fluid/solid interface [6]. Thereby the temperature at the interface between fluid and solid is not fixed but is a result of the fluid/solid thermal coupling and influenced by the state and properties of gas and liner. Hence the local liner surface temperature is an output of the calculations and will vary spatially and temporally.

RESULTS

The effect on the liner surface temperature of including CHT calculations is indicated in Figure 3 and Figure 4 for the reference case where a temperature of 50°C is imposed on the backside of the solid liner cell layer.

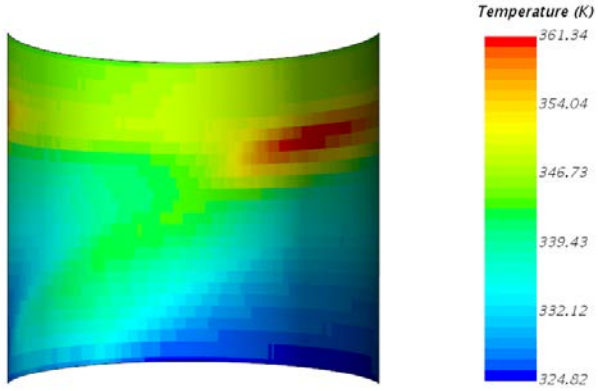

Figure 3 Liner surface temperature at 40 CAD ATDC.

An illustration of the variation obtained in the liner surface temperature when including CHT calculations in the simulation is shown in Figure 3. The figure shows the surface temperature of the liner at 40 CAD ATDC. The liner surface temperature is seen to vary up to 37K at this crank angle.

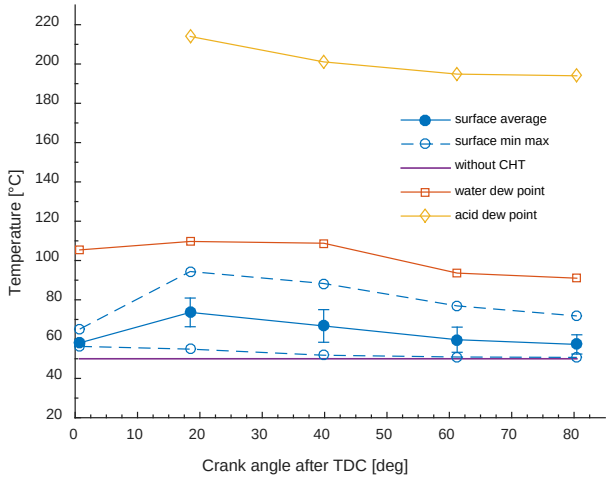

Figure 4 Effect on liner surface temperature of including CHT calculations in the reference case with dew points indicated.

The area averaged liner surface temperature $\overline{T}_w$ shown in Figure 4 is calculated according to:

$$\overline{T}_w = \frac{\sum_i T_{w,i} A_i}{\sum_i A_i} \quad (1)$$

$T_{w,i}$ and A_i are the temperature and area of the i-th liner surface cell (liner cells located below the piston are not included). The standard deviation of $\overline{T}_w$ is indicated as well as the maximum and minimum liner surface temperatures. The purple line indicates the liner surface temperature without CHT calculations included. The temperature is increased 10-20K in average when including CHT calculations for this case with peak temperatures 30-40K above the reference temperature. The calculated area averaged dew point for sulfuric acid and water vapor at the gas/liner interface are indicated in Figure 4 as well for comparison. The sulfuric acid dew point is calculated using the correlation of Verhoff and Banchero [9]:

$$\frac{1}{T_{DP,a}} = 2.276\times10^{-3} - 2.943\times10^{-5}\ln p_w - 8.58\times10^{-5}\ln p_a + 6.20\times10^{-6}\ln p_w \ln p_a \quad (2)$$

$T_{DP,a}$ is the dew point of sulfuric acid in Kelvin (K), while p_w and p_a are the partial pressures of water and sulfuric acid, respectively, in the unit millimetre of mercury (mmHg). The sulfuric acid dew point is only calculated in areas where the mole fraction of sulfuric acid is above 1 ppm. Below that threshold it is considered that the effect of potential sulfuric acid condensation will be negligible. Such areas are in the present investigation assumed to have a sulfuric acid mole fraction of zero, i.e. they are not included in the calculation of the area averaged sulfuric acid dew point. The calculation of the water dew point is based on Han et al. [10]:

$$p_w = 610.78\exp\left(17.2694\frac{T_{DP,w} - 273.15}{\left(T_{DP,w} - 273.15\right) + 238.3}\right) \quad (3)$$

$T_{DP,w}$ is the dew point of water in Kelvin (K), and p_w is the partial pressure of water in Pascal (Pa). In Figure 4, no sulfuric acid dew point is shown at 0 degrees since no sulfuric acid vapor is present at the liner surface at this time. The liner surface temperature in both the case with and without CHT calculations is observed to be well below the sulfuric acid dew point. Sulfuric acid condensation at the liner surface is therefore considered probable in both cases, and including CHT calculations seems not to change the picture. A similar situation is indicated for water vapor condensation on the liner surface. However, including CHT calculations is seen to increase the liner surface temperature predictions significantly at about 20-40 CAD ATDC relative to the water vapour dew point level when comparing to the case without CHT calculations.

The temperatures presented in Figure 4 are, as mentioned, surface area averaged values, and for the liner surface temperature, global maximum and minimum values are also indicated. Thus comparing the shown liner surface temperatures with the dew point profiles indicates if condensation is probable in general. However, it is also of interest to evaluate the actual fraction of the liner surface area which may be exposed to possible condensation and subsequently risk of corrosion attack. This is done by calculating the fraction of the liner surface (only liner cells located above the piston are considered) which has a temperature lower than the local dew point of sulfuric acid and water vapor, respectively. The surface fraction F_s is calculated according to:

$$F_s = \frac{\sum_i \phi_i A_i}{\sum_i A_i} \quad (4)$$

The parameter ϕ assumes the value 1 if the temperature of the i-th liner surface cell is below the local dew point of the considered component (sulfuric acid or water) and is zero otherwise. Results for the reference case in Figure 4 are presented in Figure 5.

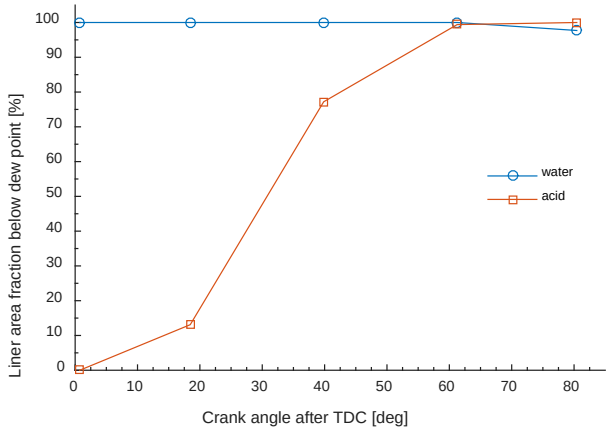

Figure 5 Fraction of liner surface area above the piston which is below dew points of water and sulfuric acid, respectively, in the reference case.

The local liner surface temperature is found to be below the dew point of water on all the liner surface above the piston, except at 80 CAD ATDC where the fraction drops to 98%. This agrees with the expectation from the results in Figure 4, and water condensation may thus potentially occur on the entire liner surface except at the late crank angle degrees. A potential sulfuric acid condensation may be expected on the entire liner surface as well based on the results in Figure 4 that indicate liner surface temperatures well below the sulfuric acid dew point. However, in Figure 5 it is observed that the fraction of the liner surface which may potentially be exposed to sulfuric acid condensation increases from zero and first reach 100% about 60 CAD ATDC. This is due to the fact that no sulfuric acid vapor is predicted at the gas/liner interface initially and first appears at the interface gradually during the combustion phase. Results for the liner surface fraction where sulfuric acid is present (above 1 ppm) give the same curve (not shown here) as the acid curve in Figure 5. Thus, where sulfuric acid is present at the gas/liner interface, the surface temperature is below the sulfuric acid dew point as expected from the results in Figure 4. If a temperature of 50°C is used to calculate the fractions in Figure 5 instead of

the actual liner surface temperature, the results indicate what the fractions would be in the case of a fixed surface temperature of 50°C, i.e. without CHT calculations included in the simulation. For the reference case, these results (not presented here) show that the liner area fractions as function of crank angle are almost identical to those in Figure 5. This indicates that including CHT calculations in the reference case has almost no influence on the predicted liner area fractions where condensation may potentially occur. This conclusion is also expected from the results in Figure 4 since the liner surface temperature is below both the sulfuric acid and water vapor dew points in general.

Next we investigate a case where the imposed thermal boundary condition on the backside of the liner cell layer is increased to 90°C in order to evaluate the effect of including CHT calculations when the thermal boundary condition is closer to the water dew point. The area averaged liner surface temperature for this case is presented in Figure 6 together with the global maximum and minimum and standard deviation values. Calculated area averaged dew points at the gas/liner interface are also included as well as the liner surface temperature without CHT calculations.

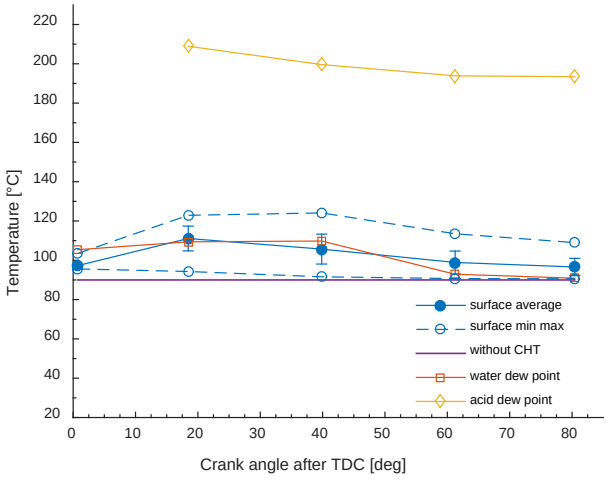

Figure 6 Effect on liner surface temperature of including CHT calculations in the case with a thermal boundary condition of 90°C.

The fixed liner surface temperature is seen to be lower than the calculated area averaged water dew point. However, when CHT calculations are incorporated, the liner surface temperature increases and is partly above and partly below the area averaged dew point for water. Thus, for this case, it is expected that when CHT calculations are included, a lower liner surface area exposed to potential water condensation will be predicted than without CHT calculations. Figure 7 shows the calculated fraction of the liner surface above the piston which has a temperature below the dew point of water and sulfuric acid, respectively. Also shown in the figure is the situation when the fraction calculations are performed with a fixed temperature of 90°C instead of the actual liner surface temperature. This represents the case when CHT calculations are not included in the simulation.

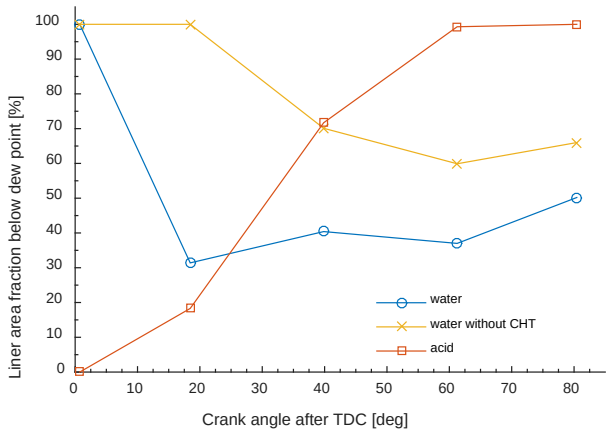

Figure 7 Fraction of liner surface area above the piston which is below dew points of water and sulfuric acid, respectively, in the case with a thermal boundary condition of 90°C.

The fraction of the liner area where condensation of sulfuric acid may potentially occur is predicted to increase from zero and up to 100% at about 60 CAD ATDC similar to the reference case. The reason for this is, as in the reference case, that sulfuric acid is not initially present at the gas/liner interface but gradually appears. Results which are not presented here show, as in the reference case, that the effect of CHT calculations on the liner area fraction, which has a temperature below the sulfuric acid dew point, is negligible for the present case. This is due to the relative large difference between the local sulfuric acid dew point and local liner surface temperature. However, when considering the results for the predicted liner area fraction, which has a surface temperature below the water dew point, the effect of including CHT calculations is significant, as evident from Figure 7. Hence in situations when the thermal boundary condition on the liner is relatively close to the dew point (in the present case within 20K) inclusion of CHT calculations are important.

The above investigations consider situations with a uniform temperature imposed on the backside of the liner cell layer. The temperature will however vary along the liner in reality. This situation is considered next where a more realistic thermal boundary condition is imposed on the backside of the liner cell layer. The imposed temperature profile is based on measurements in a large two-stroke marine diesel engine 5 mm below the liner surface. The temperature profile is a second order polynomial varying from 250°C at the cylinder cover to 48°C at the scavenge ports at the lower end of the liner and was also used by Sigurdsson et al. [7]:

$$T = 40z^2 - 180z + 523 \qquad (5)$$

T is the temperature in Kelvin (K), and z is the distance from the cylinder cover in meters (m). The results from this case are shown in Figure 8 and Figure 9.

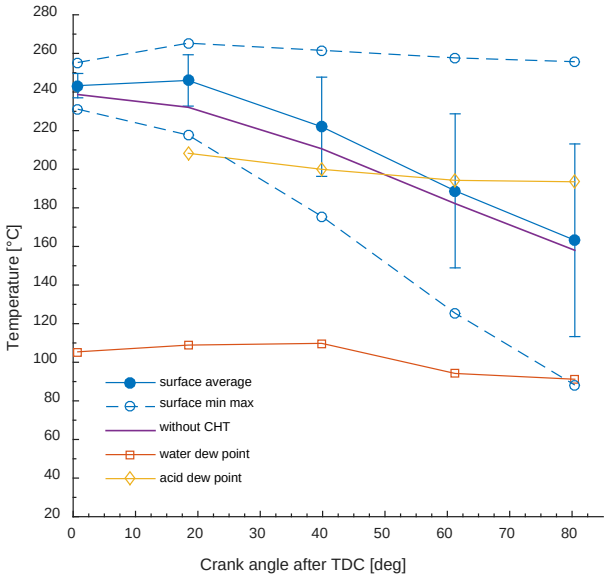

Figure 8 Effect on **l**iner surface temperature of including CHT calculations in the case with a non-uniform thermal boundary condition.

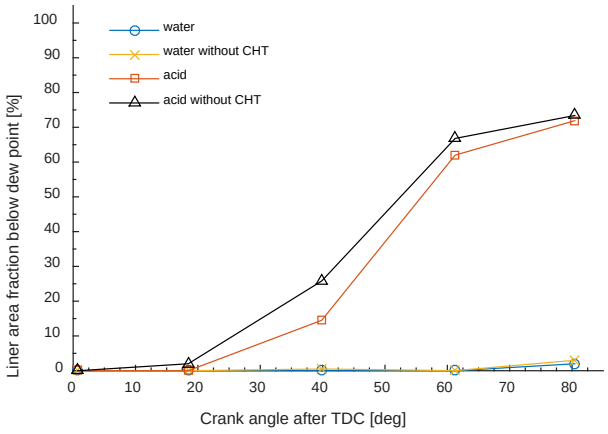

Figure 9 Fraction of liner surface area above the piston which is below dew points of water and sulfuric acid, respectively, in the case with a non-uniform thermal boundary condition.

It is observed that the liner area fraction with a surface temperature below the local water dew point is close to zero, and that inclusion of CHT calculations in this case has almost no influence on the predictions. This is also expected from the results in Figure 8 where it is seen that the area averaged liner surface temperature is significantly higher than the area averaged water dew point. The fraction of the liner surface area where sulfuric acid may potentially condense exhibits the same trend with crank angle as observed in the previously investigated cases. It does not reach 100% though since a part of the liner surface will in this case have a temperature above the sulfuric acid dew point. The predictions are observed to be influenced by the inclusion of CHT calculations in the simulation. The difference is up to about 11 percent points.

CONCLUSION

We have conducted an investigation of the effect of including conjugate heat transfer calculations in the CFD simulation of the combustion phase of a large two-stroke marine diesel engine. The effect on the liner surface temperature was observed, and the consequence for the predictions of sulfuric acid and water condensation on the liner was evaluated. An increase in the average liner surface temperature in the order of 20K was found when including CHT calculations. This was observed to affect the predictions of potential sulfuric acid and water condensation only if the liner surface temperature is near the local dew points. For a case with a realistic thermal boundary condition imposed on the liner, it was found that including CHT calculations influenced to some degree the predictions of potential sulfuric acid condensation. Predictions of potential water condensation was contrarily observed to be less influenced by the inclusion of CHT calculations since the surface temperature of a large part of the liner area was significantly higher than the water dew point.

ACKNOWLEDGEMENTS

The authors gratefully acknowledge funding from Innovation Fund Denmark and MAN Energy Solutions SE through the SULCOR project and funding from A/S D/S Orient's Fond.

REFERENCES

[1] Jorgensen R., Slow steaming – The full story, *A. P. Moller – Maersk Group*, 2011

[2] Jensen P., Bach M., Saloufas A., Tsalapatis D., and Rolsted H., Lubtronic SIP promise remarkably low wear rates with low CLO consumption, *CIMAC World Congress on Combustion Engine 28*, Helsinki, Finland, June 2016, paper 283

[3] Kjemtrup L., Cordtz R. F., Meyer M., and Schramm J., Experimental investigation of sulfuric acid condensation and corrosion rate in motored BUKH DV24 diesel engine, *Proceedings of the ASME 2017 Internal Combustion Engine Division Fall Technical Conference*, Seattle, USA, 2017

[4] Pang, K. M., Karvounis N., Walther J. H., Schramm J., Glarborg P., and Mayer S., Modelling of temporal and spatial evolution of sulphur oxides and sulphuric acid under large, two-stroke marine engine-like conditions using integrated CFD-chemical kinetics, *Applied Energy*, Vol. 193, 2017, pp. 60-73

[5] Karvounis N., Pang K. M., Mayer S., and Walther J. H., Numerical simulation of condensation of sulfuric acid and water in a large two-stroke marine diesel engine, *Applied Energy*, Vol. 211, 2018, pp. 1009-1020

[6] Siemens, STAR-CCM+ version 13.06 - User Guide, *Siemens PLM Software*, 2018

[7] Sigurdsson E., Ingvorsen K. M., Jensen M. V., Mayer S., Matlok S., and Walther J. H., Numerical analysis of the scavenge flow and convective heat transfer in large two-stroke marine diesel engines, *Applied Energy*, Vol. 123, 2014, pp. 37-46

[8] Pang K. M., Karvounis N., Walther J. H., and Schramm J., Numerical investigation of soot formation and oxidation processes under large two-stroke marine diesel engine-like conditions using integrated CFD-chemical kinetics, *Applied Energy*, Vol. 169, 2016, pp. 874-887

[9] Verhoff F. H. and Banchero J. T., Predicting dew points of flue gases, *Chemical Engineering Progress*, Vol. 70, 1974, pp. 71-72

[10] Han H., He Y. L., and Tao W. Q., A numerical study of the deposition characteristics of sulfuric acid vapor on heat exchanger surfaces, *Chemical Engineering Science*, Vol. 101, 2013, pp. 620–630